ISSN: 0067-2904

Origin of Dolomites in the Baluti Formation (Late Triassic), Galley Derash Area, N-Iraq: Petrography, Textural and Diagenetic Properties

Sa'ad Zeki A. Kader Al-Mashaikie*, Suhad Khalaf A. Razzak
Department of Geology, College of Science, University of Baghdad, Baghdad, Iraq

Abstract

Baluti Formation of the Rhaetian (Late Triassic) age is composed mainly of dolomite, the unit formed with dolomitic limestone, dolomitic breccias and limestone begins with gray or dark gray colored and sugar textured dolomitic limestones including micrite with shale horizons. Baluti Formation was deposited in carbonate platform, and slumped to deeper margins forming carbonate debrites and breccias of various types.

Petrographic examination of the dolomites reveals various crystal habits and textures of the dolomites. Planktonic bivalve, calcisphere and echinoid spicules were found in the Baluti Formation settled in deep-margin carbonate environment. Nine dolomite-rock textures were identified and classified according to the crystal-size distribution and crystal-boundary shape. These are made of unimodal, 1) very fine to fine-crystalline planar-s (subhedral) mosaic dolomite; 2) unimodal, medium to coarse-crystalline planar-s (subhedral) mosaic dolomite; 3) coarse to very coarse crystalline planar-s (subhedral) dolomite; 4) medium to coarse-crystalline planar-e (euhedral) mosaic dolomite; 5) medium to coarse-crystalline planar-e (euhedral) dolomite; 6) coarse to very coarse-crystalline non-planar-a (anhedral) dolomite; 7) coarse to very coarse-crystalline non-planar-c (cement) dolomite; 8) polymodal, planar-s (subhedral) to planar-e (euhedral) mosaic dolomite. Dolomitization is closely associated with the development of secondary porosity; dolomitization pre and post diagenetic dissolution and corrosion and no secondary porosity generation is present in the associated limestones. The most common porosity types are non-fabric selective moldic and vugy porosity and intercrystalline porosity. These porous zones are characterized by late-diagenetic coarse-crystalline dolomite, whereas the non-porous intervals are composed of dense mosaics of early-diagenetic dolomites. The distribution of dolomite rock textures indicates that porous zones were preserved as limestone until late in the diagenetic history, and were then subjected to late-stage dolomitization in a medium burial environment, resulting in coarse-crystalline porous dolomites. Baluti dolomites have been formed as early diagenetic at the tidal-subtidal environment and as a late diagenetic at the shallow-deep burial depths.

Keywords: Baluti, Gulley Derash, Dolomite, Peritidal, Petrography

*Email: magnesite2006@gmail.com

اصل الدولومايت في تكوين بلوطي (الترياسي المتأخر) في منطقة كلي ديرش شمال العراق : الصفات الصخارية والنسيجية والعمليات التحويرية

سعد زكي عبد القادر*، سهاد خلف عبد الرزاق
قسم علم الارض ، كلية العلوم ، جامعة بغداد، بغداد، العراق .

الخلاصة

يتكون تكوين بلوطي العائد لعمر الراتين (الترياسي المتاخر) اساسا من الدولومايت المتكون مع الحجر الجيري المدلمت والدولومايت بريشيا ذي اللون الرصاصي الغامق والنسيج المحبب مع طبقات من الحجر الطيني . لقد ترسبت تكوين بلوطي في هضبة بحرية جيرية وقد زحفت هذه الرواسب الى مناطق بحرية عميقة مكونة الركام الصخري البحري وانواع من البريشيا الجيرية.

تظهر الدراسات الصخرية المجهرية انواع عديدة من انسجة واشكال بلورات الدولومايت. لقد تم تمييز من المتحجرات ذات المصراعين الطافية والكالسيسفير واشواك القنافد البحرية والتي ترسبت في بيئة بحرية عميقة. لقد تم تمييز تسعة انواع من انسجة الدولومايت والتي صنفت بالاعتماد على حجم البلورات وتوزيعها وانواع الحدود البلورية . وتتكون هذه الانسجة(1) بلورات دولومايت مستوية وناعمة الى ناعمة جدا واحادية االشكل وغير متكانلة الاوجه (2) بلورات احادية الشكل متوسطة الى خشنة الحجم مستوية وغير متكاملة الاوجه (3) بلورات احادية الشكل خشنة الى خشنة جدافي الحجم مستوية وغير متكاملة الاوجه (4) بلورات احادية الشكل متوسطة الى خشنة في الحجم غير مستوية متكاملة الاوجه (5) بلورات احادية الشكل متوسطة الى خشنة في الحجم مستوية ومتكاملة الاوجه (6) بلورات خشنة الى خشنة جدا في الحجم وغير مستوية وعديمة الاوجه تكون المادة الرابطة (7) بلورات متعددة الشكل مستوية ومتكاملة الاوجه الى غير متكاملة الاوجه (8) الدولومايت المصاحب لاشنات الستروماتولاتيت.

ان عملية الدلمتة غالبا ما تكون مصاحبة لعملية تكون المسامية الثانوية في الحجر الجيري. ان انواع المسامية الثانوية تتمثل في المسامية غير النسيجية والمتواجدة في اصدارات المتحجرات والفجوات بين البلورات. تتميز منطقة المسامات هذه ببلورات الدولومايت الخشنة والمتاحره النشأة بينما تتميز المنطقة غير المسامية ببلورات دواومايت متراصة كثيفة وذات فسيفساء اولية النشأة. ان توزيع انسجة بلورات الدولومايت يشير الى ان المنطقه المسامية قد احتفظت بتكوين الحجر الجيري الى بداية العمليات التحويرية المتأخرة وعندها تتأثر بالعمليات التحويرية المتأخرة النشاءة في بيئة متوسطة العمق مكونة بلورات دولومايت خشنة تملأ المسامات لذا فأن الدويومايت في تكوين بلوطي قد تكون بنشأة متقدمة في بيئة المد البحري وتحتها وكنشأة متأخرة في اعماق ضحلة الى عميقة.

Introduction

Baluti Formation is one of Triassic stratigraphic units, which are very little studied. It is of Late Triassic age, and is cropping out in a narrow valley inside Jabal Gara Mountain (Figure-1). Previous works represented field observations in the study area [1] were generally aimed to elucidate the general geology of the area. No previous investigation of petrographic characteristics of dolomites found in the Baluti beds. The carbonate rocks are still to investigate in detail. Various mechanisms for the formation of dolostone in platform carbonates have been summarized by [2] Among these hypotheses, dolomitization related to hypersaline brines, mixed meteoric and sea water, and deep basinal brine have found almost acceptance. The only major source of magnesium for penecontemporaneous and shallow-burial dolomitization may be seawater [3, 4]. Magnesium for deep burial conditions can be supplied from (a) trapped seawater (connate waters); (b) dissolution of unstable minerals; (c) pressure solution (stylolitization); (d) compaction of underlying shales; and (5) basinal brines. The basinal brines are the most likely magnesium source for dolomitization [4]. In case of combined thermodynamic and kinetic parameters, the following environmental conditions are responsible for dolomitization: (1) environments of any salinity above thermodynamic and kinetic saturation with respect to dolomite (i.e. freshwater/seawater mixing zones, normal saline to

hypersaline subtidal environments, hypersaline supratidal environments, schizohaline environments); (2) alkaline environments (i.e. those under the influence of bacterial reduction and/or fermentation processes, or with high input of alkaline continental groundwater); and (3) many environments with temperatures greater than about 50^0C (subsurface and hydrothermal environments) [5]. Sometimes, the dolomites are not macroscopically observed in the field, where different types of dolomites are easily distinguished by petrographic examination and scanning electron microscopy (SEM). It was observed that Baluti Formation is composed of grey and yellowish drab limestones.

The aim of this study is to examine the micro textural characteristics, diagenetic development and origin of the dolomites in the Baluti Formation.

Geology and stratigraphy

The suggested age of the Baluti Shale (as formerly named) is Late Triassic (Rhaetian). The Baluti beds composed of 60 m gray to green shales with thin bedded dolomitic, silicified and oolitic limestones and breccias (Figure- 2). The formation is cropping out in Ranya area in NE Iraq [6,7,8], and two shale units are reported in Serwan gorge SE Halabjah city. In other areas of Iraq, a unit of limestone, anhydrite and subordinate shales is usually referred to Baluti Shale Formation [1, 9] but lacks the high proportion of shale seen in the outcrops [10]. The thickness of the formation is around 35-60 m at the outcrops. It was identified in the subsurface drilled wells; Jabal Kand-1 (61 m), Khlessia-1 (22 m), Atshan-1 (40 m) and W Kifl-1 (46 m). In well Dewan-1 was not identified, being either included within the Kurra Chine Formation or Butmah Formation. The formation is thinning westwards. Both lower and upper contacts of the formation are conformable (Bellen et al., 1959) except in well Tharthar-1 [10]. Because of lack of diagnostic fossils, age of the formation was determined from stratigraphic position between Upper Triassic Kurra Chine Formation and the overlying Sarki Formation (Liassic) [1], where lagoonal/evaporitic and estuarine are the suggested environment of deposition. Equivalent formations in western Iraq may be eroded. [11] assumed that the Zor Hauran Formation is tentatively correlated with the Baluti Formation [10].

Methodology

The study of Baluti Formation based and used data-base of 25 samples collected from non-previously studied stratigraphic section from Galley Derash Valley in Jabal Gara Mountain in Amadiya area, N Iraq (Figure- 1). Twenty-three (23) thin section slides along the section of the Baluti Formation were cutting perpendicular to the bedding plane followed the procedure listed in [12]. The thin sections are stained by alizarin red-S solution to distinguish calcite from dolomite [13]. Carbonate rocks are classified according to [14] system modified by [15]. Five grinding powdered samples are tested by Scanning Electron Microscopy (Zeiss 50 VP) equipped with an Energy Dispersive X-Ray Spectroscopy (Oxford Instruments Inca Energy) at the department of physics Science at the Collage of Sciences at Kufa University.

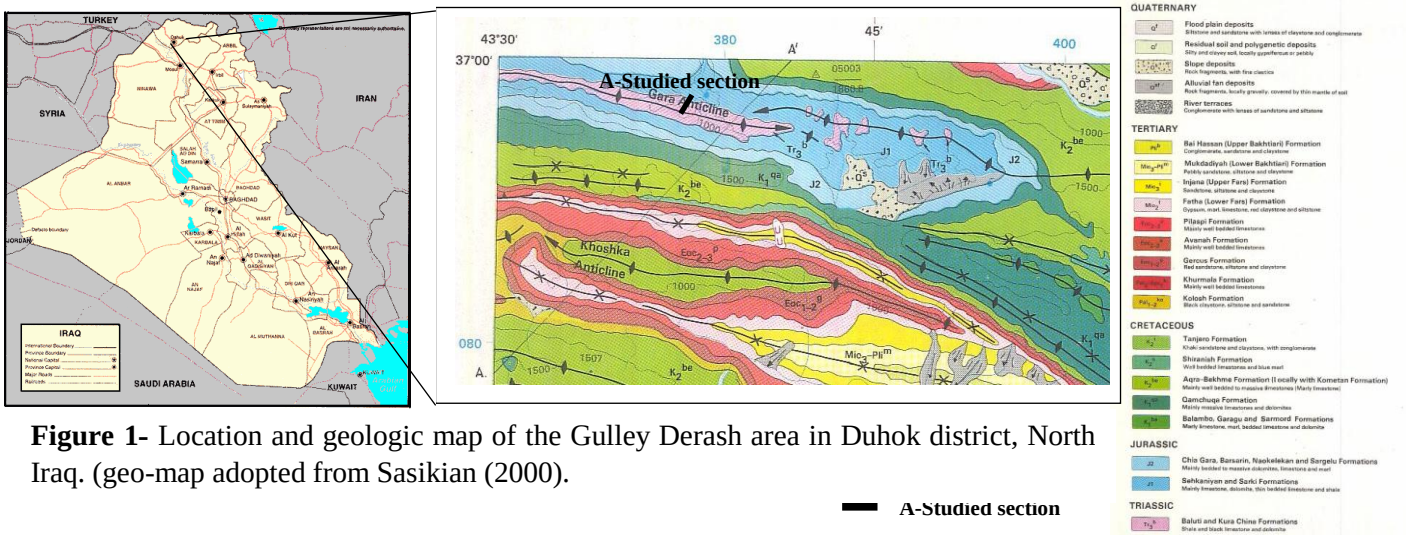


Figure 1- Location and geologic map of the Gulley Derash area in Duhok district, North Iraq. (geo-map adopted from Sasikian (2000).

A-Studied section

Sarki

10m interbedded thin beds of dark gray fragmented shales and pale brown to drab brecciated limestones

1.5m Carbonate breccia with stromatolite fragments, dark gray in color
3m Laminated dolomitic limestone, drab to dark gray in color with carbonate fragments
1.5m Black fissile shale with carbonate and organic matter

6m successive interbedded yellow to drab dolomite/limestone with organic matter

1.5m Massive, dark gray shale bed
2m Dolomite, dark gray, massive

12m Interbedded dark grey (1-2m) with yellow to drab beds of dolomitic limestone (1-2.5m), successive cycles
3m Limestone, yellow, thin bedded with occasional dolomite.

1.5m Shale, thick massive bed

4m Sandstone, gray, slump and disturbed thick bed with fragments of stromatolite

5m Carbonate breccia, thick massive and yellowish bed, includes little shale fragments

2m Fragmented shale, dark gray, composed of pebble size fragments of shale

5m Carbonate breccia with olistolith, bedded, yellowish to dark gray color

1.5m Dolomitic limestone, massive, gray to yellow color
2m fissile shale, thick bed and dark gray in color

3m Carbonate breccia, massive, yellow in color with channel structure

2m fissile shale, thick bed and dark gray in color

3mDolomitic limestone and shale interbeds, dark to light gray and yellow color
5m Shale bed, laminated, dark gray, with fissility property

2m Interbedded fine-grained carbonate breccia with limestone, yellow, thin bedded

2m Fragmented shale, small pebble size fragments, black to dark gray, massive bed

Figure 2- Stratigraphic section of the Baluti Formation in Galley Derash area, Duhok area N-Iraq.

Dolomite-rock textures

Petrography

Seven dolomite-rock textures have been recognized and classified according to crystal-size distribution (unimodal or polymodal) and crystal-boundary shape (planar or non-planar), using the dolomite-rock classification scheme of [16-19]. The classification is descriptive with genetic implications, in which the size distribution is controlled by both nucleation and growth kinetics. Moreover, the crystal-boundary shape is controlled by growth kinetics [16, 20].

In this study, the classification of dolomite-rock textures is based on petrographic studies supported by analysis of scanning electron microscope (SEM) images.

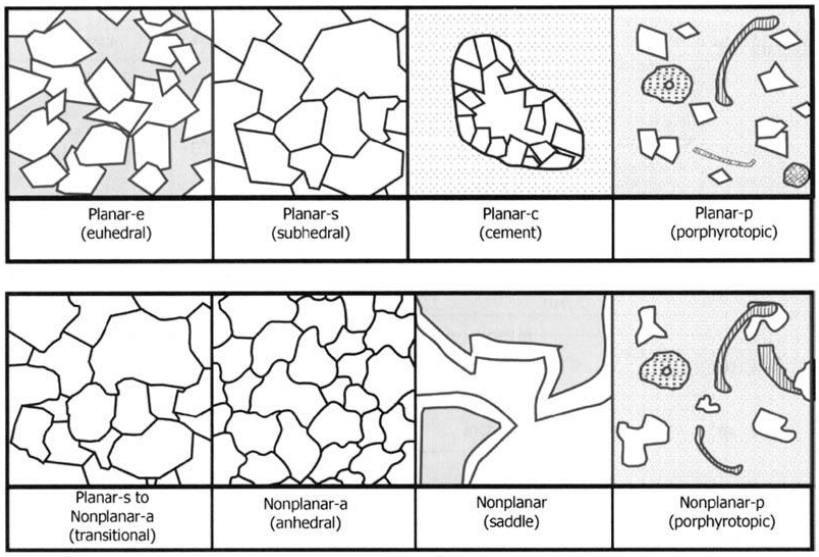


Figure 3- Dolomite textural classification combined from [18, 16] supplemented by a 'transitional' form. The figure is reproduced with permission from [21].

The following dolomite-rock textures have been defined: (1) unimodal, very fine- to fine-crystalline planar-s (subhedral) mosaic dolomite, (2) unimodal, medium- to coarse-crystalline planar-s (subhedral) mosaic dolomite, (3) coarse- to very coarse-crystalline non-planar- to planar-c (cement) dolomite, (4) medium- to coarse-crystalline planar-e (euhedral) mosaic dolomite, (5) stromatolitic dolomite, (6) non-planar-a (anhedral), coarse to very coarse-crystalline, and (7) Polymodal planar-s (subhedral) to planar-e (euhedral) Mosaic dolomite (Plate/1, Figures- 4 to 9).

Dolomite texture 1: unimodal, very fine- to fine-crystalline planar-s (subhedral) mosaic dolomite

This type represents the first phase of replacive dolomites that have planar-s texture. Typically, the dolomites consist of scattered crystals of <20 μm in diameter in a micrite matrix groundmass (Plate/1-A). The dense very fine mosaics show no recognizable allochems, but in some times preserved sedimentary structures (laminae) can be observed. An alteration of very fine-crystalline (dark) with fine-crystalline (clear) dolomite laminae is very common in the laminated dolomudstone/wackestone facies. In places, patches of fine-crystalline calcite occur within the fine-crystalline mosaic dolomite.

Dolomite texture 2: unimodal, medium- to coarse-crystalline planar-s (subhedral) mosaic dolomite

This type comprises dense mosaics of subhedral to anhedral planar-s (subhedral) crystals (80-250 μm). These dolomite crystals are cloudy core with clear rim texture to totally cloudy crystals (Plate/1-B). The most characteristic feature is the non-mimic replacement of allochems (ooids, peloids, intraclasts, fossils and fossil-fragments). These allochems can be recognized as ghost textures (Plate/1-G pellets). In this type, it is difficult to recognition the original depositional textures. SEM analysis shows the presence of medium to-coarse crystalline, planar-s dolomite rhombs (Figure- 6). In the SEM (Figure- 6), the dolomite appears slightly dissolved. The EDX spectrum indicates the presence of (Ca, Mg) major elements as typical of dolomite Figures-(4, 5).

Dolomite texture 3: Coarse to very coarse-crystalline planar to non-planar-c (cement) dolomite

This type of texture reveals coarse to very coarse-crystalline (150-1500 μm) dolomite cement (Plate/1-C, J). The boundary between the dolomicrite and some of the dolomite rhombs are mottled. The most petrographic character is the milky-white to clear crystals with sweeping extinction under crossed Nichols. Under plane polarized light, triangular surface irregularities may be observed, as well as curved crystal faces. Planar-c dolomite type present to lines the vugs and fractures and occurs as major void-filling dolomite. Thus, it is responsible for occlusion of pore spaces and fractures.

Dolomite texture 4: Medium- to coarse-crystalline planar-e (euhedral) mosaic dolomite

In this type of texture, the dolomite crystals make mosaics of mostly planar-e, medium- to coarse-crystalline (60-600 μm) dolomite (Plate/1-D). The crystals are clear to cloudy textures. No replacement textures are observed. This type is filling the interior of replaced fossil shells, makes up the mottled parts in the mottled dolo-mudstone facies, is responsible for sucrose dolomites in breccias, and occurs near stylolite. SEM analysis shows the presence of coarse to-very coarse crystalline, planar-e rhombic dolomite Figures-(6, 8). In the SEM (Figure- 6), the dolomite appears slightly dissolved. The EDX spectrum indicates the presence of Ca and Mg major elements of typical of dolomite (Figure- 7).

Dolomite texture 5: Stromatolitic dolomite

This type of dolomite texture consists of mimetic replacement of stromatolite in the limestone rocks (Plate/1-E). It is also fills the pores of the stromatolite with dolomite crystals and in the same cases the calcite cement was replaced by dolomite. This type forms dense mosaics of subhedral to anhedral planar-s crystals (10-100 μm). The crystals of dolomite are milky white, clear, or have a cloudy core with clear rim texture or vice versa.

Dolomite Texture 6: non-planar-a (anhedral), coarse to very coarse-crystalline

This type of texture comprises dense and tightly packed mosaics of coarse to very coarse-crystalline non-planar-a dolomite crystals (Plate/1-F). The crystals have irregular, serrated, curved or otherwise indistinct boundaries. The crystals show vague non-mimetic replacement. Preserved crystal faces are rare or absent.

Dolomite texture 7: Polymodal planar-s (subhedral) to planar-e (euhedral) Mosaic dolomite.

This type comprises replacement dolomite, which attains polymodal planar-euhedral to planar-subhedral crystals. The crystal size distribution is ranging between 50 and 750 μm (Plate/1-G). The centers of the rhombs are cloudy and surrounded by clear zone. Some of the rhombs show clear sugar habit, and other rhombs are cutting across by micro-stylolite.

Dolomite texture 8, Mosaic dolomite. Polymodal planar-s (subhedral) to planar-e (euhedral)

This type comprises replacement dolomite, which attains polymodal planar-euhedral to planar-subhedral crystals. Crystal size distribution is ranges between 50 and 750 μm (Plate/1-H). The centers of the rhombs are cloudy and surrounded by clear outer zone. Some of the rhombs show clear sugar habit, and some of the rhombs are cutting across by micro-stylolite.

Dolomite texture 9, Mosaic dolomite. Non-planar-p (porphyrotopic)

This type comprises replacement and cementing dolomite, which attains non-planer coarse crystals surrounded by small crystals groundmass. Crystal size distribution is ranges between 50 and 750 μm (Plate/1-J, I). The crystals are clear and some skeletal grains are embedded within.

Petrographic interpretation

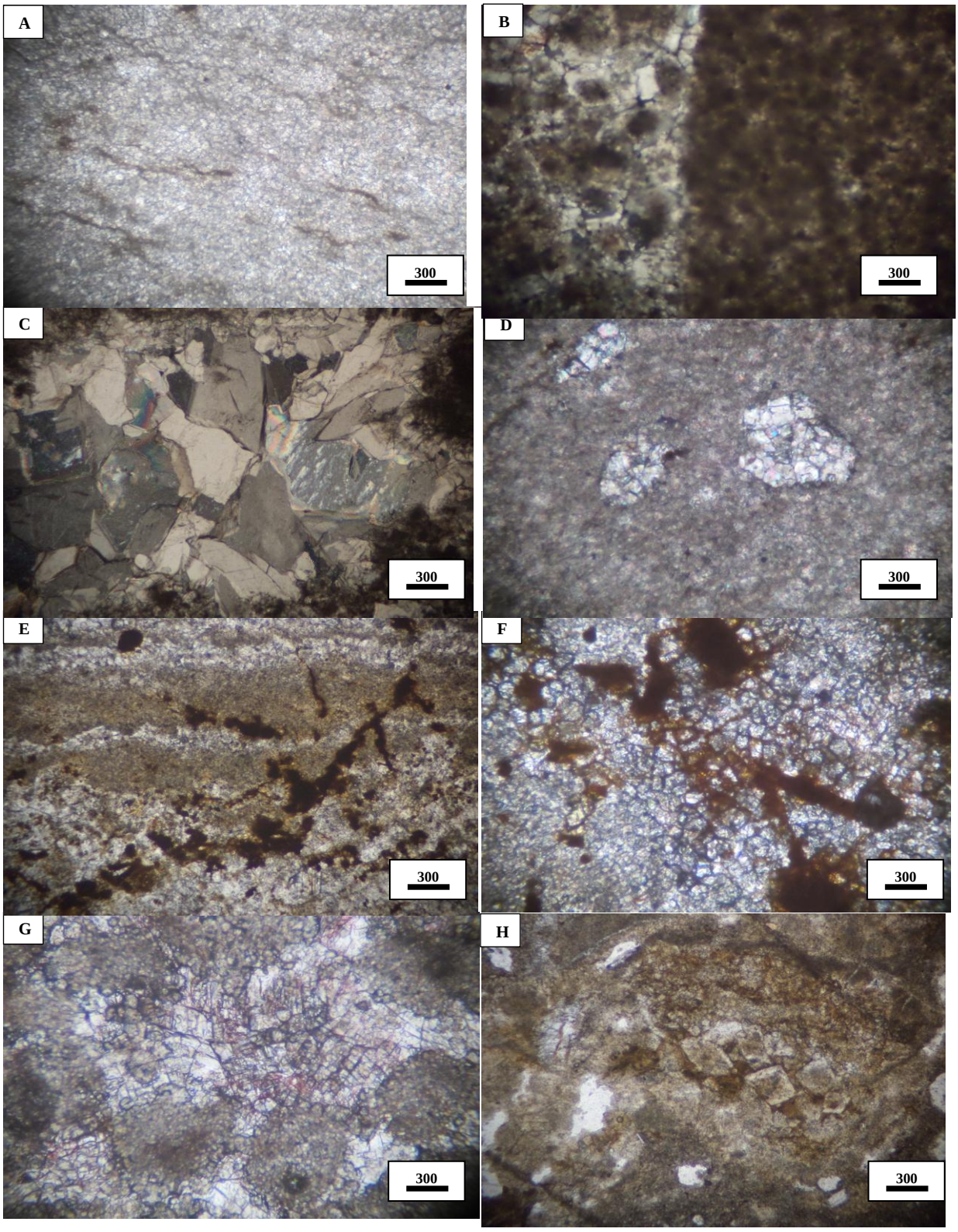
Dolomite fine crystal size may form by early replacement of peritidal lime mudstones and/or neomorphism of syndepositional or early diagenetic dolomite [20, 22-25]. The formation of fine-crystalline (<50 m), planar-s (subhedral) type 1 dolomite is associated with evaporites, typical of arid peritidal sequences and/or subtidal/supratidal settings. These dolomites replace open-marine intraclasts and bioclastic packstones and grainstones [25-30].

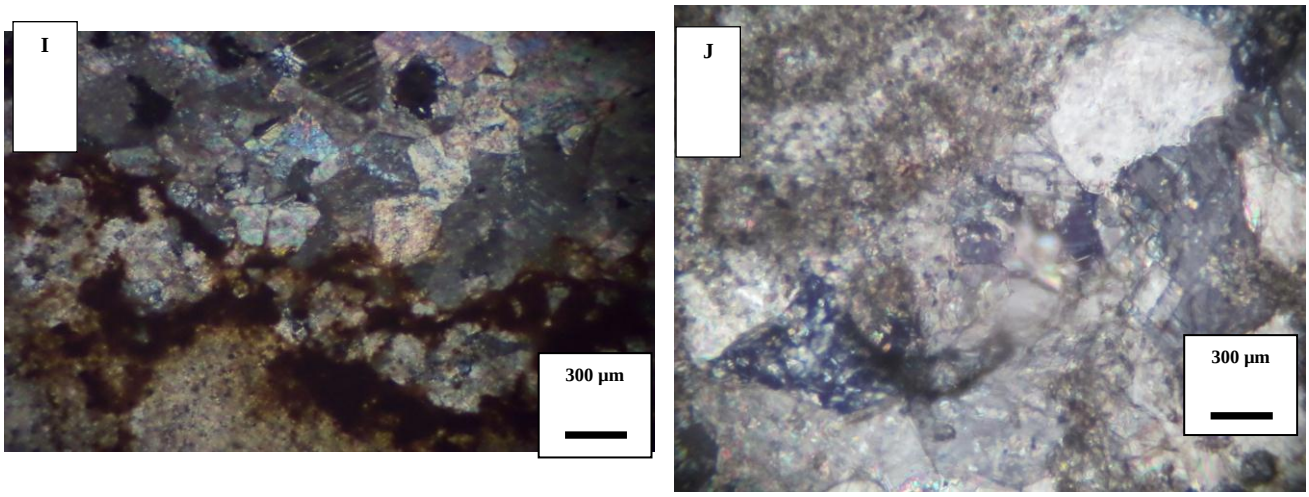
The rate of nucleation and rate of growth are controlling the crystal size habits. Very fine dolomite crystals are of very large surface areas in comparison to their volume and therefore, rapid nucleation rates were formed. Therefore, the high nucleation rate compared to the growth rate is resulted fine crystal size [20, 24, 3].

Experimental data of [16] reported that increases of dolomite formation results increase crystal size. This indicates selective dolomitization of finer crystalline calcium carbonate and early dolomitization of subtidal to supratidal lime muds [20, 23-27, 29, 30]. These data are interpreting the dolomite type 1 as early diagenetic dolomite and/or synsedimentary formation [23, 31]

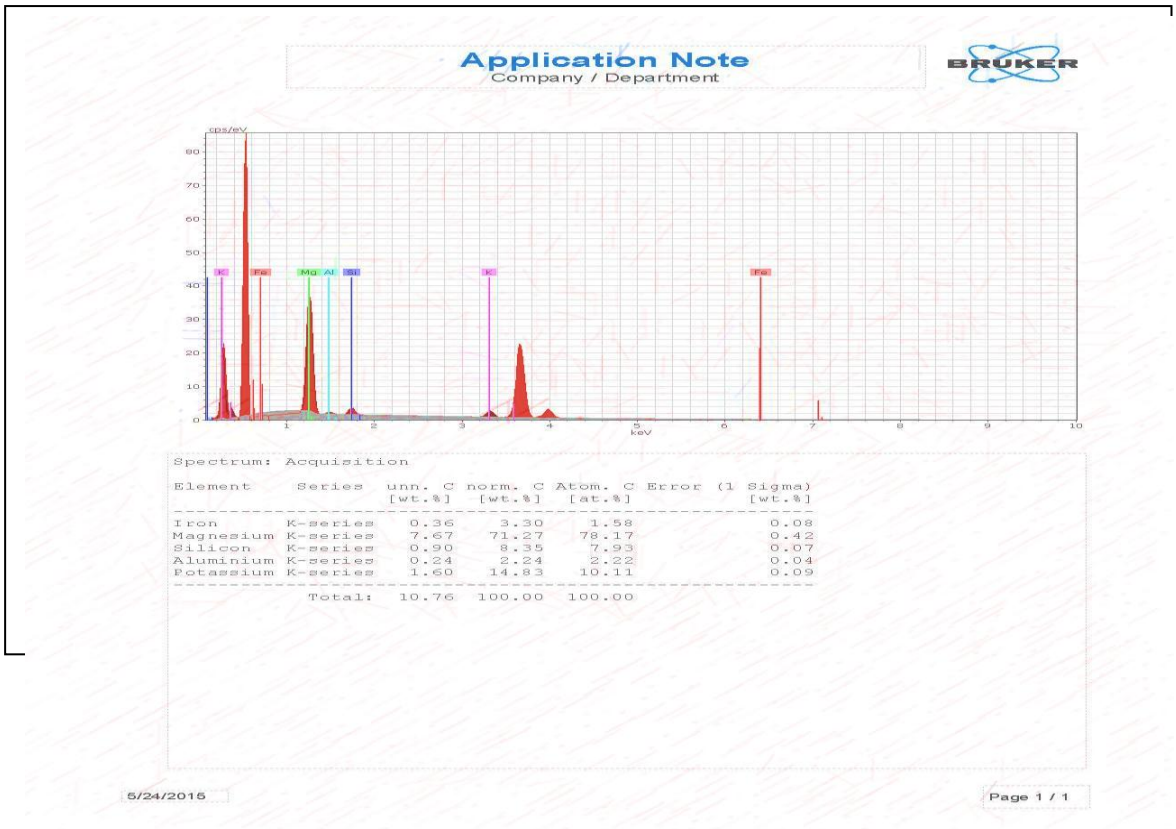
replacing subtidal to intertidal carbonate mud. Based on paragenetic relationships, the dolomite type 2 to 8 is interpreted as intermediate to late diagenetic replacement dolomites.

PLATE/1





Plate/ 1. Microphotographs show types of dolomite textures in the Baluti Formation.
1. Type-1, unimodal, very fine- to fine-crystalline planar-s (subhedral) mosaic dolomite. **B)** Type-2, unimodal, medium- to coarse-crystalline planar-s (subhedral) mosaic dolomite. **C)** Type-3, Coarse- to very coarse-crystalline planar- to non-planar-c (cement) dolomite. **D)** Type-4, Medium- to coarse-crystalline planar-e (euhedral) mosaic dolomite. **E)** Type-5, Stromatolitic dolomite. **F)** Type-6, non-planar-a (anhedral), medium to coarse-crystalline. **G)** Type-7, Polymodal planar-s (subhedral) to planar-e (euhedral) Mosaic dolomite. **H)** Type-8, Mosaic dolomite. Polymodal planar-s (subhedral) to planar-e (euhedral). **I and J),** Type-9, Mosaic dolomite. Non-planar-p (porphyrotopic).



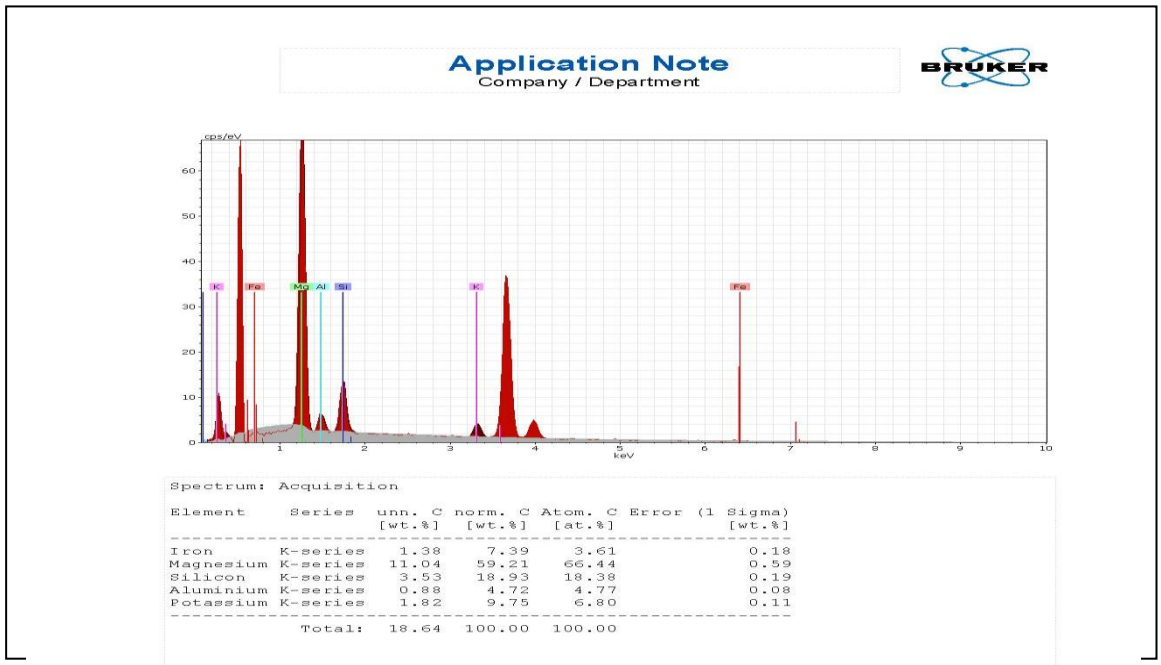


Figure 5- Energy dispersive X-Ray Spectrum (EDX) shows medium to coarse crystalline planar-s dolomite (dark gray) rhombs.

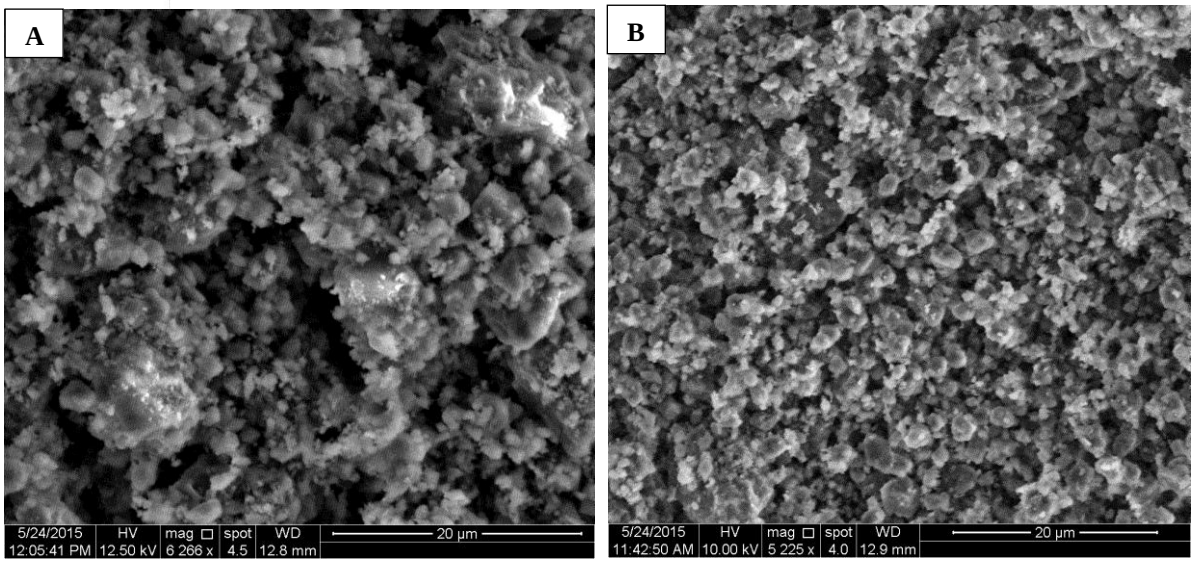


Figure 6- SEM photomicrograph shows, A) fine to medium crystalline planar-e dolomite (dark gray) rhombs B) fine crystalline planer-e dolomite.

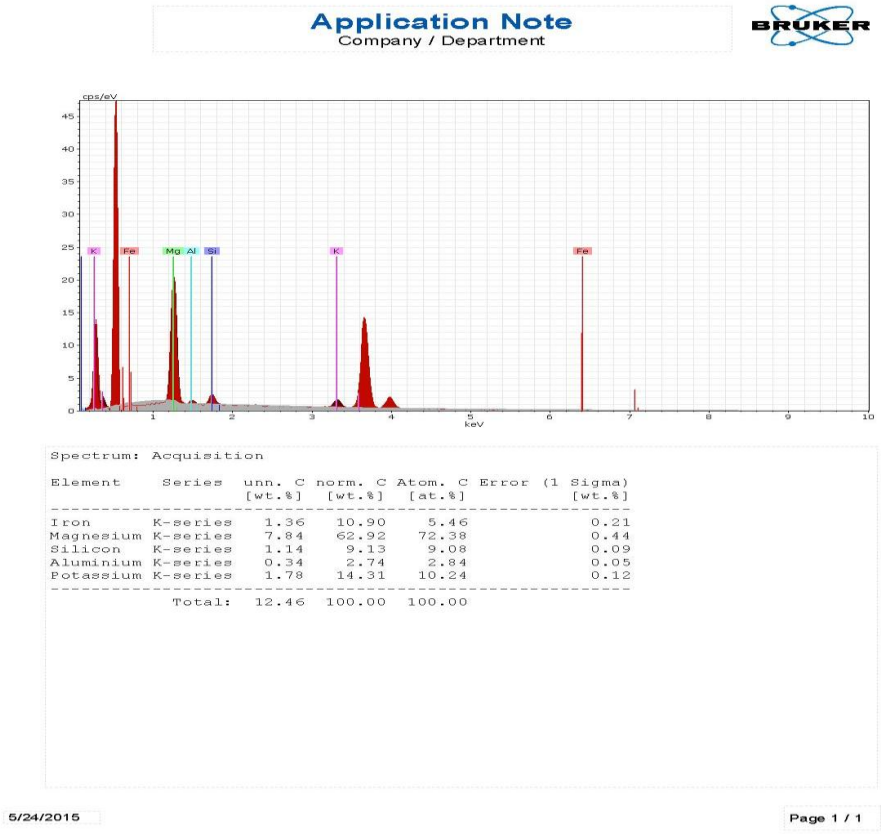


Figure 7- Energy dispersive X-Ray Spectrum (EDX) shows medium to coarse crystalline planar-e dolomite (dark gray) rhombs.

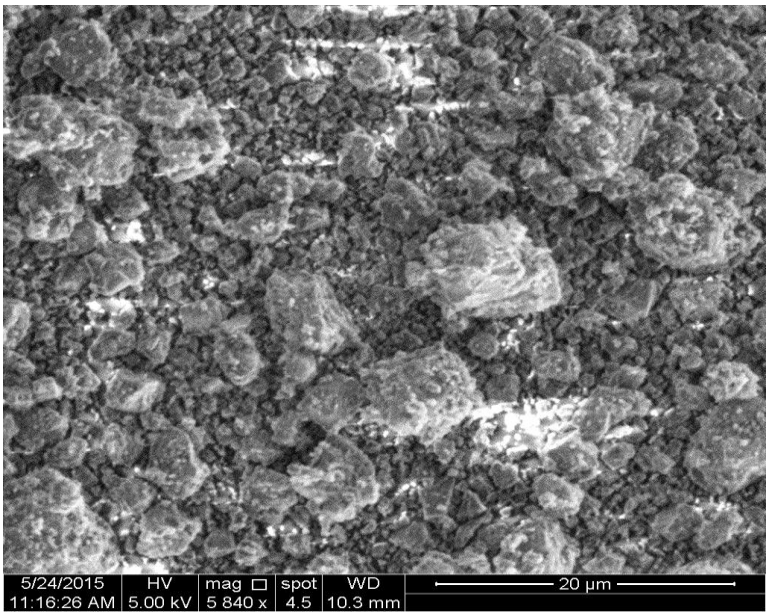


Figure 8- SEM photomicrograph shows medium to coarse crystalline planar-e dolomite (dark gray) rhombs (SEM), and energy dispersive X-Ray Spectrum (EDX).

The preservation of original depositional textures and the coarse crystal size suggest major and probably long later dolomitization events. This type compares in part to dolomite type 3 of [4] and compares to the dolomite type 2 of [32, 20], which interpreted to originate during late burial origin. The main characteristic feature of dolomite type 2 is the cloudy core, clear rim texture, which is common in rocks of all ages [33, 20] and non-mimetic replacement of allochems. Cloudy cores represent replacive dolomite, whereas the clear rims are zoned dolomite cements that occupied intercrystalline porosity [20, 24]. Preserved primary sedimentary fabric needs volumetric rate of dolomite growth, equal to the volumetric rate of calcite dissolution [34, 20]. This refers to host-phase dissolution and precipitation must occur simultaneously along with thin solution film [35, 34, 20, 23]. This type comprises dolomite cement and dolomite replacing precursor cement. The term void-filling dolomite [16] is employed for this type, because it is often not possible to differentiate between dolomite cement and dolomite replacing precursor cement. Dolomite type 3 occurs together with dolomite types 1 and 2. Paragenetic relationships indicate that dolomite 3 is of later origin than dolomite 1 and contemporaneous (replacive dolomite) or later (cement) than dolomite 2.

The planar-e mosaics dolomite texture does not give much evidence of the original texture. It can be assumed that the dolomite nucleation sites are homogeneously distributed because of the unimodal crystal size in individual mosaics [33, 36, 20, 31]. The dolomite crystals are shared compromise boundaries, indicating that they formed in situ. They grow simultaneously to form compromise crystal boundaries and planar-e mosaics by coalescence growth [36] of zones in adjoining crystals [20]. The lack of intracrystalline truncation features, the continuity and equal width of zones indicate continuous growth of the crystals [20]. Dolomite type 4 occurs as a matrix in collapse breccias. It is also forms mosaics in the dolo-mudstone, which is encountered within the fossil shells and replaced later by dolomite type 2. These paragenetic relationships indicate an intermediate to late diagenetic origin, which is associated with significant intercrystalline porosity [26, 27, 29, 30].

The planar-e of medium to coarse crystalline, selective replacive dolomites are generally selectively replaced the fine crystalline calcium carbonates e.g. limestone [16, 20]. The finer particles have very large surface areas and, therefore rapid nucleation rates are formed. The high rates of nucleation in comparison to the growth rate results small crystal size. The formation of medium to coarse crystal sizes dolomites suggest replacement in fine crystalline calcite or dolomite originated in shallow-medium burial late diagenetic processes. The preservation of original textures of coarse crystal size suggests a major and probably long late dolomitization of late burial origin [20, 26, 27, 29-31].

Dolomite type 5 is characterized by cloudy core and clear rim texture, which is common in rocks of all ages [33, 20] with mimetic replacement of allochems (Plate/1-A). The presence of intercrystalline truncation in the dolomite rhombs are indicated dissolution later than dolomitization. Late diagenetic filling crack with saddle dolomites are occurred at elevated temperatures (burial origin and/or hydrothermal solutions) in the faulted carbonate breccias, which are cut across dolomite type 5. The euhedral form of saddle dolomite rhombs suggests formation at temperatures below 50-100^0 C (critical roughening temperature) since higher temperatures favor anhedral forms [16, 26, 27, 37, 29, 30].

Non-planar-a dolomite occurs as replacement of precursor limestones or dolostones and it is usually obliterating all original textures [20, 29]. This type corresponds to the xenotopic-a dolomite as defined by [18, 16]. They propose that the xenotopic dolomite texture is resulted from the replacement of dolomite or by neomorphic recrystallization of pre-existing dolomites at elevated temperatures [18, 20, 31].

It was recognized the non-planar-a dolomite type is replacing precursor limestones in a burial environment. Such replacement took place only in zones of original high porosity and permeability. This coarse non-planar dolomite cement is usually termed saddle dolomite [20, 29], and mostly interpreted to form at elevated temperatures (60- 150^{0}C) and from high-salinity brines [29,31].

These evidences interpret that the non-planar type-c dolomite has formed at elevated temperatures from brines in higher salinity seawater [20]. The Polymodal size distributions may develop from heterogeneous nuclei distribution, multiple time periods of nucleation, or rate variations in the local growth [16]. The original rock of high porosity and planar crystals is tending to form euhedral crystals of planar-e type (Plate/1-H). The original rocks of low porosity and planar dolomite is tending to form subhedral to anhedral crystals of planar-s type (Plate/1-C) [16, 26, 27, 29, 30].

Genesis of dolomite

The origin of magnesium in shallow-burial dolomitization is probably come from seawater [3, 4]. Magnesium for deep-burial environments is most probably supplied from (a) trapped seawater (connate waters, (b) disintegration of unstable minerals, (c) pressure solution diagenesis (stylolitization), (d) overburden pressure of underlying shales, and (e) basinal brines [4, 38, 39, 40, 41]. The thermodynamic and kinetic parameters suggest the following conditions of environments to chemically conducive dolomitization:

(1) Salinity conditions to form dolomite in response to thermodynamic and kinetic saturation e.g. normal saline/hypersaline subtidal environments, mixing zones of freshwater/seawater, supratidal hypersaline and schizohaline environments) (2) Alkalinity of the sea water e.g. with high input of alkaline continental groundwater, influence of bacterial reduction and/or fermentation processes. (3) Temperatures higher than 50^0 C c.f. subsurface and hydrothermal solutions [5]. The main sources of diagenetic fluids are meteoric, seawater and deep basinal brines.

Previous workers such as [4, 41, 42-50] noted that burial diagenetic alteration of illite and smectite led to release metal ions to provide the pore fluids. It is well documented that the basinal shale act as a source of Ca, Fe, Mg, Na and Si during deep burial diagenesis. Smectite is typically tend to release the Fe^{2+} and Mg^{2+} ions at high temperatures of transformation [41]. The smectite-illite transformation is carried out at temperature of 50 to 125^0 C and burial depths of 2-4 km in normal geothermal gradients [41]. Similarly, siliciclastic rocks e.g. shales, are suggested to give the metal ions needs to dolomitization [51].

Several suggestions are sited for the fluid mechanism in response to tectonic activities of the gravity driven fluids, episodic dewatering of basinal sediments with fluid flows [41,42].

Mahboubi et al., [52] refer that the concentrations of Fe^{2+} and Mn^{2+} ions in the meteoric water is lower than Na^+ and K^+. the increases of Fe^{2+} and Mn^{2+} ions with decreases of Na^+ ion is probably related to reducing of organic matter, which is supported by positive correlation observed between Fe^{2+} and Mn^{2+}. Dolomitization process is possibly take place in environment rich in organic matter and associated with positive correlation between Fe^{2+} and Mn^{2+} ions in the dolomites [51]. Intense dolomitization possibly formed in shallow subtidal of moderate to high hypersaline environment [5]. Dolomites in mixing-zone, is probably developed extensively during major regressive periods in the carbonate platform. The regression of sea is accompanied with progradation of the meteoric-marine mixing zone. The active circulation of water in the carbonate sediments, reflect extensive effect of climate in this model [53].

The principal mechanism of this model is the compactional dewatering of basinal mud rocks and associated expulsion of Mg^{2+} rich fluids into adjacent shelf-edge of the carbonate platform. The source of Mg^{2+} ions is the pore water and clay mineral transformation. The composition of subsurface fluids is not well known but in fact many formational waters have low Mg/Ca ratios (1.8-0.04) than seawater (5.2) [53]. The low Mg/Ca ratio is mainly being come from the formation of chlorite and of dolomite formation during shallow burial stage. It is well documented that the transformation of clay minerals in increasing burial depth is associated with increases temperature. It is frequently suggested that Mg^{2+} along with Fe^{2+}, Ca^{2+}, Si^{4+} and Na^+ are released during the transformation of smectite to illite, while Ca^{2+} and Si^{4+} are releasing in the early stage of diagenesis to precipitate the calcite cement and authigenic quartz, and the Fe^{2+} and Mg^{2+} in later stage [53]. The black shales in the Baluti Formation is commonly rich in organic matter c.f. basinal shales, and the diagenesis of organic matter could have contributed $CO3^{-2}$ [53].

Otherwise, dolomitization is proceeding more easily at depth with higher temperatures.

[54] has been found out stratified stromatolite and planktonic bivalve fossils in the Baluti Formation. Existence of the stromatolite fossils suggest that carbonate sediments is deposited in shallow-marine carbonate platform. The presence of planktonic bivalve is characteristic of deeper marine margin, suggests that the Baluti sediments are slumped to deeper margins. In conclusion, the dolomite of the Baluti Formation has been formed as early diagenetic at the tidal-subtidal environment and in late diagenetic at the shallow-deep burial depths.

Conclusion

Unimodal, very fine to fine-crystalline planar-s (subhedral) mosaic dolomite is interpreted as early-diagenetic dolomite replacing subtidal to intertidal carbonate muds. Unimodal, medium to coarse-crystalline planar-s (subhedral) mosaic dolomite is interpreted to represent intermediate to late-

diagenetic replacement dolomite. Coarse to very coarse-crystalline planar-s (subhedral) dolomite is later than dolomite 1 and contemporaneous (replacive dolomite) or later (cement) than dolomite 2. Medium to coarse-crystalline planar-e (euhedral) mosaic dolomite occurs as matrix of collapse breccias, it forms mosaics in the burrowed dolomudstone facies, and it is encountered within fossil shells that were replaced by dolomite type 2. The medium to coarse size formation in medium to coarse-crystalline planar-e (euhedral) replacement dolomites suggests fine crystalline calcite or dolomite replacement originated from shallow-medium burial late diagenetic processes. Coarse to very coarse-crystalline non-planar-a (anhedral) dolomite was occurred as replacement of a precursor limestone or dolostone. Coarse to very coarse-crystalline non-planar-c (cement) dolomite is usually termed saddle dolomite formed at elevated temperatures from basinal brines with higher salinities than seawater. Polymodal, planar-s dolomite formed probably by non-mimetically replacement of unimodal matrix and allochems. Polymodal, planar-e dolomite was occurred by dissolution of undolomitized matrix and allochems. The shales and siliciclastic of the Kurra Chine Formation, which is conformability lies in the bottom of Baluti Formation could have provided the ions required for the dolomitization of Baluti formation. Dolomites have been formed as early diagenetic at the tidal-subtidal environment and of late diagenetic at the shallow-deep burial depths.

References

1. Bellen, R.C.V., Dunnington, H.V., Wetzel, W., and Morton, D.M. **1959**. *Lexique stratigraphique international, Asie Fasc. 10a, Iraq*: Centre Natl. Recherche Sci. Paris 333 p.
2. Hardie, L. A. **1986**. Dolomitization. A critical view of some current wiev-perspectives, *Jour. Sed. Petrol.*, **57**: 166-183.
3. Land, L.S. **1985**. The Origin of Massive Dolomite, *Jour. Geol. Educ*., **33**: 112-125.
4. Lee, Y. I. and Friedman, G. M. 1987. Deep-Burial Dolomitization in the Lower Ordovician Ellenburger Group Carbonates in West Texas and Southeastern New Mexico, *Jo. Sed. Petrol*., **57**: 544-557.
5. Machel, H.G. and Mountjoy, E. W. **1986**. Chemistry and Environments of Dolomitization-A Reappraisal, *Earth. Sci. Rev.*, **23**: 175-222.
6. Wetzel, R. **1950**. Stratigraphy of Amadia region. MPC report No.IR/WR 12. Manuscript report, GEOSURV, Baghdad.
7. Buday, T. **1980**. *The regional geology of Iraq, Volume 2, Tectonism, Magmatism and Metamorphism*. Publication of GEOSURV, Baghdad. 352p.
8. Bolton, C.M.G. **1955**. Geological map-Kurdistan series, Scale 1:100,000 sheet K4 Ranya. Site. Inv. Co. Report, Library, No. 276, Baghdad.
9. Ditmar, V. and Iraqi-Soviet Team. **1971**. Geological conditions and hydrocarbon prospects of the Republic of Iraq (Northern and Central parts). Manuscript report, INOC Library, Baghdad.
10. Jassim, S.Z. and Goff, J.C. **2006**. *Geology of Iraq*. Dolin Prague and Moravian Museum. Brno, Czech Republic, 341p.
11. Buday, T. **1980**. *The regional geology of Iraq, Volume 1, Stratigraphy and paleontology*. In Kassab I.M., and Jassim S.Z., eds., (in collaboration with staff members and experts of the State Organization for Minerals, Baghdad). Directorate General of Geological Survey and Minerals. 445p.
12. Tucker, M.E. **1988**. *Technique in Sedimentology*. Blackwell scientific publication,394 p.
13. Scholle, P.A., and Ulmer – Scholle, D.S., **2003**. A Color Guide to Petrography of the Carbonate Rocks: Grains, Texture, Porosity, and Digenesis Tulsa, Oklahoma, USA: *AAPG Memoir* **77**, 474 p.
14. Dunham, R.J. **1962**. Classification of carbonate rocks according to their depositional texture. In Ham W.E, ed., Classification of carbonate rocks: Tulsa, OK, *AAPG*, Memoire1, p. 108-121.
15. Embry, A. F. and Kolvan, J. E. **1971**. Late Devonian reef tract on northeastern bank island, N.W.T.: *Bulletin of Canadian Petroleum Geology*, **19**: 730-781.
16. Sibley, D.F. and Gregg, J.M. **1987**. Classification of dolomite rock textures. *J. Sed. Petrol*, **57**(6): 967--975
17. Sibley, D. F., **1982**. The Origin of Common Dolomite Fabrics Clues from the Pliocene. *Jour. Sed. Pet.*, **52**(4): 1087-1100.

18. Gregg, J. M. and Sibley, D. F. **1984**. Epigenetic Dolomitization and the Origin of Xenotopic Dolomite Texture, *Jour. Sedim. Petrol.*, **54**: 908-931.
19. Sibley, D.F. **2003**. Dolomite textures. *In*: Middleton, G.M., Church, M.J., Conglio, M.,Hardie, L.A.and Longstaffe, F.S. (eds) *Encyclopedia of Sediments and Sedimentary Rocks*. Kluwer, Dordrecht, pp: 231–234.
20. Amthor, J. E. and Friedman, G. M. **1991**. Dolomite-Rocks Textures and Secondary Porosity Development in Ellenburger Group Carbonates (Lower Ordovician), West Texas and Southeastern New Mexico, *Sedimentology*, **38**: 343-362.
21. Wright, V. P. **1984**. Peritidal Carbonate facies models: a review. *Geological Journal*, **19**: 309 - 325.
22. Zenger, D. H. and Dunham, J. B. **1980**. Concept of models of dolomitization-an introduction, *Geol. Soc. Econ. Paleont. Miner. Spec. Publ*., **28**: 1-119.
23. Gregg, J.M., Howard, S.A. and Mazzullos, S. **1992**. Early diagenetic recrystallization of Holocene (< 3000 years old) peritidal dolomites, Ambergris Cay, Belize. *Sedimentology*, **39**: 143-160.
24. Woody, R.E., Gregg, J.M. and Koederitz, L.F. **1996**. Effect of Texture on Petrophysical Properties of Dolomite: Evidence from the Cambrian-Ordovician of Southeastern Missouri. *AAPG Bulletin*, **80**(1): 119–132.
25. Read, JF., Husinec, A., Cangialosi, M., Loehn, CW., Prtoljan, B. **2016**. Climate controlled fabric destructive, reflux dolomitization and stabilization via marine- and synorogenic mixed fluids: An example from a large Mesozoic, calcite-sea platform, Croatia. *Palaeogeography, Palaeoclimatology, Palaeoecology*, **449**: 108–126.
26. Compton, J.S., Hall, D.H., Mallinson, D.J. and Hodell, D.A. **1994**. Origin of dolomite in the phosphatic Miocene Hawthorn Group of Florida. *Jo. Sed. Research*, July, **64**, (3a).
27. Ehrenberg, S.N. G. P. Eberli. G.P. Keramati, M. Moallemi, S.A. **2006**. Porosity-permeability relationships in interlayered limestone-dolostone reservoirs. *AAPG*, January, **90** (1): 23-35.
28. Nagy, Zs.R., Gregg, J.M., Shelton, K.L., Becker, S.P., Somerville, I.D. and Johnson A.W., **2004**. *Early dolomitization and fluid migration through the Lower Carboniferous carbonate platform in the SE Irish Midlands: implications for reservoir attributes*. In Braithwaite Raithwaite, C. J. R., Rizzl G. and Darke, G. (eds) **2004**, *The Geometry and Petrogenesis of Dolomite Hydrocarbon Reservoirs*. Geological Society, London, Special Publications, 235p, pp: 367-392.
29. Merino E, Canals A, and Fletcher RC. **2006**. Genesis of self-organized zebra textures in burial dolomites: Displacive veins, induced stress, and dolomitization. *Geologica Acta*, 4(3): 383-393.
30. Vlahovic, I., Tisljar, J., Fucek, L., Ostric, N., Prtoljan, B., Velic, I. and Maticec, D. **2002**. The origin and Importance of the dolomite-limestone breccia between the Lower and Upper Cretaceous deposits of the Adriatic carbonate platform: An example from Cicarija Mt. (Istria, Croatia). *Geologia Croatica*, 55(1): 45-55.
31. Rameil, N. **2008**. Early diagenetic dolomitization and dedolomitization of Late Jurassic and earliest Cretaceous platform carbonates: A case study from the Jura Mountains (NW Switzerland, E France). *Sedimentary Geology* 212(1-4): 70-85.
32. Mattes, B. W. and Mountjoy, E. W. **1980**. *Burial dolomitization of the Upper Devonian Miette Buildup*, Jasper National Park, Alberta. In Zenger D. H., Dunham J. B. and Ethington R. L. (eds.): *Concepts and models of dolomitization*, 259-297. *SEPM Memoire*, Tulsa.
33. Woody, R.E. Gregg, J.M. and Koederitz L.F. **1996**. Effect of Texture on Petrophysical Properties of Dolomite: Evidence from the Cambrian-Ordovician of Southeastern Missouri. *AAPG Bulletin*, **80**(1): 119–132.
34. Dockal, J. A. **1988**. Thermodynamic and Kinetic Description of Dolomitization of Calcite and Calcitization of Dolomite (dedolomitization), *Carbonates and Evaporites*, **3**: 125-141.
35. Chen, D. Qing, H. and Yang, H. **2004**. Multistage hydrothermal dolomites in the Middle Devonian (Givetian) carbonates from Guilin area, South China. *Sedimentology* (2004), **51**: 1029-1051.
36. Schofield, K. **1984**. Are Pressure Solution, Neomorphism and Dolomitization Genetically Related? In: Stylolite and Associated Phenomena-Relevance to Hydrocarbon Reservoirs, *Spec. Publs Abu Dhabi Nat. Reservoir Res. Found.*, 183-201.
37. Hood, S. D., Nelson, C. S. and Kamp, P. J. J. **2004**. Burial dolomitisation in a Non-Tropical Carbonate Petroleum Reservoir: the Oligocene Tikorangi Formation, Taranaki Basin, *New Zeland, Sedim. Geol*., **172**: 117-138.

38. Teedumae, A., Shogenova, A. and Toivo Kallaste, T. **2006**. Dolomitization and sedimentary cyclicity of the Ordovician, Silurian, and Devonian rocks in South Estonia. Proc. *Estonian Acad. Sci. Geol.*, 2006, **55**(1): 67-87

39. Xiang, G. Pingkang, W. Dairong, L. Qiang, P. Chengshan, W. and Hongwen, M. **2012**. Petrologic characteristics and genesis of dolostone from the Campanian of the SK-I Well Core in the Songliao Basin, China. *GEOSCIENCE FRONTIERS*, **3**(5): 669-680.

40. Li, W. Beard, BL. Li, C. Xu, H. Johnson, CM. **2015**. Experimental calibration of Mg isotope fractionation between dolomite and aqueous solution and its geological implications. *Geochimica et Cosmochimica Acta*, **157**: 164–181.

41. Li, FB. Teng, FZ. Chen, JT. Huang, KJ. Wang, SJ. Lang, XG. Ma, HR. Peng, YB. Shen, B. **2016**. Constraining ribbon rock dolomitization by Mg isotopes: Implications for the 'dolomite problem'. *Chemical geology* Jun 2016.

42. Burns, SJ. Mckenzie, JA. Vasconcelos, C. **2000**. Dolomite formation and biochemical cycles in the Phanerozoic. *Sedimentology*, **47** (Suppl. 1): 49-61.

43. McHargue, TR, and Price, RC. **1982**. Dolomite from clay in argillaceous or shale-associated marine carbonates. *Jour. Sed. Petrology*, **52**: 873-886.

44. Kantorowicz, J. **1984**. The nature, origin and distribution of authigenic clay minerals from middle Triassic-Jurassic Ravenscar and Brent Group Sandstones. *Clay Minerals*, **19**: 359-375.

45. Goodchild, M.W. and McD. Whitaker, J.H. **1986**. A petrographic study of the Rotliegendes sandstone reservoir) Lower Permian) in the Rough Gas Field. *Clay Minerals*, **21**: 459-477.

46. Gregg, J.M. Shelton, K.L. Johnson, A.W. Ian, D. Somerville, D. and Wayne, R. Wright, W.R. **2001**. Dolomitization of the Waulsortian Limestone (Lower Carboniferous) in the Irish Midlands. *Sedimentology*, **48**: 745-766.

47. Humphreys, B. Smith, S.A. and G. E. Strong, G.E. **1989**. Authigenic chlorite in Late Triassic sandstones from the central graben, North Sea. *Clay Minerals*, **24**: 427-444.

48. Pollastro R.M. **1993**. Considerations and applications of the illite/smectite geothermometer in hydrocarbon-bearing rocks of Miocene to Mississippian age. *Clays and Clay Minerals*, **41**(2): 119-133.

49. Essene, E.J. and D. R. Peacor, D.R. **1995**. Clay mineral thermometry: a critical perspective. *Clays and Clay Minerals*, **43**(5): 540-553.

50. Moore, D.E, and Lockner, D.A. **2007**. Friction of the Smectite Clay Montmorillonite, A Review and interpretation data. In Dixon, T. and Moore, C, eds., *Seismogenic Zone of Subduction Thrust Faults*. Columbia University Press, pp: 317-345.

51. Özkan, A.M. and Elmmas, A. **2009**. Petrographic Characteristic of the Kızıloren Formation (Upper Triassic-Lower Jurassic) in the Akpınar (Konya - Turkey) Area. Ozean *Journal of Applied Sciences*, **2**(4): 22-34.

52. Mahboubi, A. Moussavi-Harami, R. Brenner, R. L. and Gonzalez L. A. **2002**. Diagenetic History of Late Paleocene Potential Carbonate Reservoir Rocks, Kopet-Dagh Basin, NE Iran, *Jo. Petrol. Geol.*, **25**: 465-484.

53. Tucker, M. E., and Wright, V. P., **1990**, *Carbonate sedimentology*: Oxford U. K., Black well Scientific Publication, 482p.

54. Al-Mashaikie, et al., (**2016**). Sedimentology of the Baluti Formation in the Galley Derash, Amadiya, North Iraq; New carbonate turbidite facies and depositional environment. *Arabian Journal of Geosciences*, **9**: 723: 1-14.